Vol. 107 (2005) ACTA PHYSICA POLONICA A No. 5

Proceedings of the 35th Polish Seminar on Positron Annihilation, Turawa, Poland 2004

Defects in Ultra-Fine Grained Mg and Mg-Based Alloys Prepared by High Pressure Torsion Studied by Positron Annihilation

J. Čížek[a], I. Procházka[a], B. Smola[a], I. Stulíková[a], R. Kužel[a], Z. Matěj[a], V. Cherkaska[a], R.K. Islamgaliev[b] and O. Kulyasova[b]

[a]Faculty of Mathematics and Physics, Charles University in Prague
V Holešovičkách 2, 180 00 Praha 8, Czech Republic
[b]Institute of Physics of Advanced Materials
Ufa State Aviation Technical University, Ufa 450000, Russia

Despite the favourable strength and thermal stability, a disadvantage of the Mg-based alloys consists in a low ductility. Recently it has been demonstrated that ultra fine grained metals with grain size around 100 nm can be produced by high pressure torsion. A number of ultra fine grained metals exhibit favourable mechanical properties consisting in a combination of a very high strength and a significant ductility. For this reason, it is highly interesting to examine microstructure and physical properties of ultra fine grained Mg-based light alloys. Following this purpose, microstructure investigations and defect studies of ultra fine grained pure Mg and ultra fine grained Mg–10%Gd alloy prepared by high pressure torsion were performed in the present work using positron annihilation spectroscopy combined with X-ray diffraction, TEM observations, and microhardness measurements. Positrons are trapped at dislocations in Mg and Mg–10%Gd alloy deformed by high pressure torsion. A number of dislocations increases with the radial distance r from the centre to the margin of the sample. No microvoids (small vacancy clusters) were detected. Mg–10%Gd alloy deformed by high pressure torsion exhibits a homogeneous ultra fine grained structure with a grain size around 100 nm and high dislocations density. On the other hand, pure Mg deformed by high pressure torsion exhibits a binomial type of structure which consists of "deformed regions" with ultra fine grained structure and a high dislocation density and dislocation-free "recovered regions" with large grains. It indicates a dynamic recovery of microstructure during high pressure torsion processing.

PACS numbers: 78.70.Bj, 79.60.Jv, 61.72.–y

1. Introduction

Lightweight Mg-based alloys enable us to increase the effectiveness in automotive and air industries and in structural applications, which leads to a lower consumption of the fossil fuels and other energetic sources. However, the applicability of magnesium alloys is limited due to their low melting temperature T_m. A failure of the construction units can happen at temperatures higher than $0.4-0.5T_m$, i.e. 100–200°C. There is a big effort in materials science to extend the applicability of Mg-alloys to higher temperatures. The particularly promising way is the use of rare earth alloying elements [1]. For example Mg–Gd system represents a promising novel hardenable material with a high creep resistance even at elevated temperatures [2]. Despite the favourable strength and thermal stability, disadvantage of Mg-based alloys with rare earth elements consists in a low ductility, which is not sufficient for industrial applications. Thus, attempts to increase ductility of these alloys are highly desirable. Grain refinement is a well-known method how to increase ductility of metallic materials. Recently it has been demonstrated that ultra fine grained (UFG) metals with a grain size around 100 nm can be produced by high pressure torsion (HPT) [3]. A number of UFG metals exhibit favourable mechanical properties consisting in a combination of very high strength and a significant ductility. For this reason, it is highly interesting to examine microstructure and physical properties of UFG Mg-based light alloys. Following this purpose, microstructure investigations and defect studies of pure UFG Mg and UFG Mg–10%Gd alloy were performed in the present work.

2. Experimental

The specimens of Mg (technical purity) and Mg–10%Gd alloy were studied. The Gd content is given in the weight percents. We chose Mg–Gd alloy because of its promising mechanical properties and thermal stability [2]. The alloy was prepared from the technical purity Mg by squeeze casting. The as-cast material was subjected to homogenization annealing at 500°C for 6 h finished by rapid quenching in water at room temperature. In addition, a well-annealed high purity Mg (99.95%) and Gd (99.9%) were used as reference specimens. The UFG samples were prepared from the coarse grained initial materials by HPT at room temperature up to the true logarithmic strain $\varepsilon = 7$ under high pressure of 6 GPa [3]. The HPT deformed samples were disk shaped with diameter of 12 mm and thickness of 0.3 mm. A fast–fast positron lifetime (PL) spectrometer similar to that described in [4] with the timing resolution of 170 ps (FWHM ^{22}Na) at the coincidence counts rate of 120 s^{-1} was employed in the present work. A ^{22}Na positron source with activity of 1.5 MBq sealed on 2 μm thick mylar foil was used. Decomposition of PL spectra into exponential components was performed using a maximum likelihood procedure [5]. The PL measurements were accompanied by theoretical calculations of positron lifetimes using the atomic superposition (ATSUP) method [6]. TEM

observations were performed on the JEOL 2000 FX electron microscope operating at 200 kV. X-ray diffraction (XRD) studies were carried out with the aid of XRD7 and HZG4 (Seifert-FPM) powder diffractometers using Cu K_α radiation. The microhardness Hv was measured by the Vickers method with a load of 100 g applied for 10 s using the LECO M-400-A hardness tester.

3. Results and discussion

3.1. Coarse grained materials

The reference high purity Mg sample exhibits a single-component PL spectrum with lifetime $\tau_1 = 227$ ps, see the Table. It exhibits a reasonable agreement with calculated Mg bulk lifetime $\tau_B = 233$ ps. On the other hand, PL spectrum of the as-received Mg consists of two components listed in the Table. The lifetime τ_1 of the shorter component corresponds to free positrons, while the second one $\tau_2 = 256$ ps comes from positrons trapped at defects. The lifetime τ_2 lies between the Mg bulk lifetime τ_B and the calculated lifetime of positrons trapped at Mg-monovacancy $\tau_v = 297$ ps. It is typical of dislocations. Dislocation density $\rho \approx 5 \times 10^{12}$ m^{-2} and the mean grain size of about 10 μm were estimated by TEM in this specimen. Thus, we conclude that positrons are trapped at dislocations introduced into the as-received Mg during casting and shaping. In order to check experimentally this interpretation, a technical purity Mg sample was cold rolled to a thickness reduction $\varepsilon = 40\%$. The second component in the cold rolled sample exhibits indeed virtually the same lifetime τ_2 (see the Table), but a significantly higher intensity due to a higher dislocation density. Annealing the as-received Mg at 280°C for 30 min leads to a complete recovery of dislocations reflected also by a remarkable decrease in microhardness Hv (the last column of the Table). The annealed sample exhibits a single component PL spectrum with lifetime which agrees reasonably with that of the reference specimen. The reference high purity Gd sample exhibits a single-component PL spectrum with lifetime of 201 ps. It is in very good agreement with the calculated lifetime of free positrons in Gd $\tau_B^{Gd} = 204$ ps.

PL spectrum of the homogenized Mg–10%Gd alloy is well fitted by two components given in the Table. The first component with the lifetime $\tau_1 < \tau_B$ can be attributed to free positrons, while the second one with the lifetime τ_2 comes from positrons trapped at defects. TEM investigations of this sample revealed large coarse grains and a low dislocation density below $\approx 10^{12}$ m^{-2}, which approaches the lower sensitivity limit of PL spectroscopy [7]. Therefore, positrons trapped at dislocations cannot represent a noticeable contribution to PL spectrum. The component represents rather a contribution of positrons trapped in quenched-in excess vacancies "frozen" in the sample due to the rapid quenching. This interpretation is supported by the lifetime $\tau_2 \approx 300$ ps, which agrees well with the calculated lifetime of positrons trapped in Mg-monovacancy. As free monovacancies are not stable in Mg at room temperature [8], the observed defects represent

TABLE

Lifetimes and corresponding relative intensities of the exponential components resolved in PL spectra (except of the source contribution). The PL results for HPT deformed materials correspond to the centre of the sample. Microhardness values Hv are shown in the last column. In case of HPT deformed samples Hv in the centre and at the margin of the sample are given. The errors (one standard deviation) are given in parentheses.

Sample	τ_1 (ps)	I_1 (%)	τ_2 (ps)	I_2 (%)	Hv (MPa)
high purity Gd, well-annealed	201.3(5)	100	–	–	
high purity Mg, well-annealed	227.0(5)	100	–	–	
Mg as-received	204(4)	63(1)	256(1)	37(1)	440(40)
Mg annealed 280°C/30 min	225.3(4)	100	–	–	330(20)
Mg cold rolled	160(10)	14(4)	257(2)	86(4)	
Mg–10%Gd homogenized	220(4)	90.9(6)	301(9)	9.1(7)	680(30)
HPT Mg	188(5)	39(1)	257(3)	61(1)	570(30)–620(30)
HPT Mg–10%Gd	210(3)	34(2)	256(3)	66(2)	1670(40)–2330(40)

vacancies bound to Gd atoms. The coincidence Doppler broadening (CDB) ratio curves (with respect to pure defect-free Mg) for homogenized Mg–10%Gd alloy and the reference pure Gd sample are plotted in Fig. 1. Clearly the CDB profile for Mg–10%Gd reproduces well features of the profile for pure Gd, i.e. a maximum at $8 \times 10^{-3} m_0 c$. It indicates that some fraction of positrons annihilates with electrons from the electron shells of Gd atoms. The CDB ratio curve for Mg–10%Gd sample can be reasonably approximated by a fraction of about 10% of positron annihilations with Gd electrons plotted in Fig. 1 by the solid line. The CDB profile ρ of the homogenized Mg–10%Gd sample can be expressed as a sum of two contributions

$$\rho = (1-\eta)\rho_{\mathrm{f}} + \eta\rho_{\mathrm{t}}, \tag{1}$$

where ρ_{f} and ρ_{t} denote the CDB profile corresponding to positrons annihilating from the free and the trapped state, respectively. The fraction of positrons, η, annihilating from the trapped state can be calculated from PL results using expression

$$\eta = \frac{I_2\left(\tau_{\mathrm{B}}^{-1} - \tau_{\mathrm{v}}^{-1}\right)}{\tau_{\mathrm{B}}^{-1} - I_2\tau_{\mathrm{v}}^{-1}}, \tag{2}$$

where τ_{B} represents Mg bulk lifetime, τ_{v} and I_2 denote lifetime and intensity, respectively, of positrons trapped at quenched-in vacancies. We obtained $\eta \approx 2.5\%$

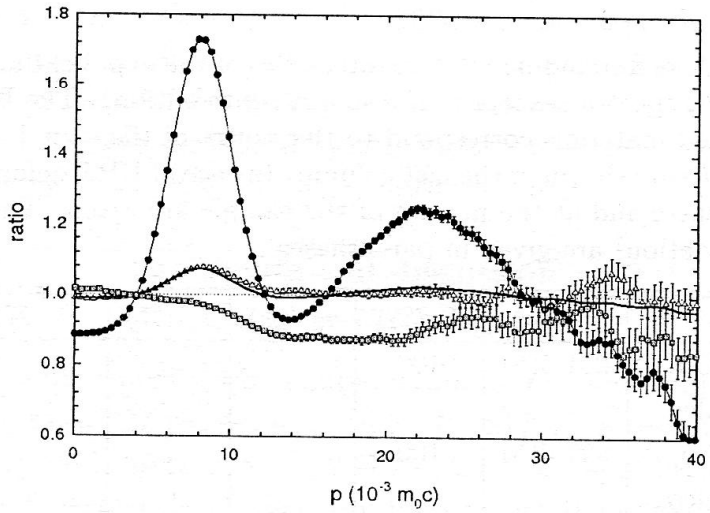

Fig. 1. The CDB ratio profiles (with respect to defect-free pure Mg) of Mg–10%Gd alloy samples. Full circles — well-annealed pure Gd, open triangles — homogenized Mg–10%Gd alloy, the thicker solid line shows a fraction of about 10% of positron annihilating with Gd electrons, gray squares — HPT deformed Mg–10%Gd alloy.

for the homogenized Mg–10%Gd sample. Thus, the 10% contribution of annihilations with Gd electrons measured by CDB cannot be explained only by contribution of trapped positrons. It is necessary to assume that $\approx 7.5\%$ of free positrons annihilates with Gd electrons as well. It is remarkably higher than the atomic concentration of Gd in Mg–10wt.%Gd alloy, which amounts only 1.6 at.%. It indicates a strong preferential positron annihilation with Gd electrons.

3.2. HPT deformed samples

A representative TEM image of the HPT deformed Mg specimen is shown in Fig. 2a. Two different kinds of regions were observed: (i) "deformed regions" with UFG grains (100–300 nm) and a high dislocation density, and (ii) "recovered regions" with substantially larger grains (≈ 1 μm) and almost free of dislocations. The presence of the "recovered regions" indicates some kind of dynamic recovery of microstructure during the HPT processing. The XRD back-reflection pattern is a superposition of isolated spots and continuous diffraction rings, which testifies co-existence of the two kinds of regions. The sample shows a texture of (001) type. No significant broadening of XRD profiles was detected so that the dislocation density should be less than about 1×10^{13} m^{-2}. However, a major contribution to the diffraction peaks comes from the "recovered regions" so that the "deformed regions" cannot be well characterized by XRD. The PL spectrum of the HPT deformed Mg consists of the free positron component and a contribution of positrons trapped at dislocations. The lifetime τ_2 of the latter component agrees well with that found in cold rolled Mg for positrons trapped at dislocations. Hence, we can conclude that positrons are trapped at dislocations inside the "deformed regions". A typical TEM image of HPT deformed Mg–10wt.%Gd

alloy is shown in Fig. 2b. It shows a uniform UFG microstructure with the mean grain size of about 100 nm, i.e. no dynamic recovery took place during the HPT processing. The electron diffraction pattern testifies high-angle misorientation of neighbouring grains. A high density of homogeneously distributed dislocations

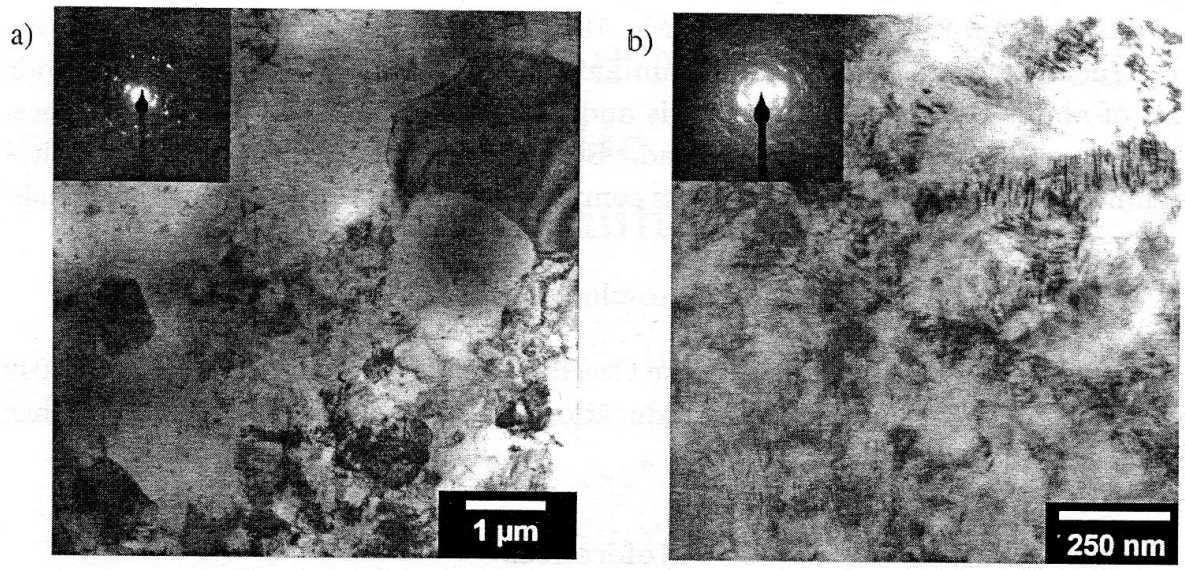

Fig. 2. Bright-field TEM image of (a) Mg and (b) Mg–10%Gd alloy deformed by HPT.

was observed. It is reflected also by a significant broadening of XRD profiles. A lower broadening of (00l) profiles with respect to other peaks indicates a dominating presence of dislocations with Burgers vector $\boldsymbol{b} = 1/3.\mathrm{a}.[2\bar{1}\bar{1}0]$. A weak (001) texture was found. The PL spectrum of the HPT deformed Mg–10%Gd alloy consists of two components, see the Table. The first component with the lifetime τ_1 comes from free positrons. The lifetime τ_2 of the second component corresponds well with that of positrons trapped at Mg-dislocations. One can see in the Table that I_2 is comparable for both HPT deformed samples despite the fact that HPT deformed Mg exhibits a remarkably lower dislocation density. This surprising effect might be explained by a smaller specific positron trapping rate for dislocations in Mg–10%Gd alloy, where mainly partial dislocations are present due to a lower stacking fault energy. However, this problem remains still open and requires additional investigations. It was found that dislocation density increases with the radial distance from the centre to the margin of the specimen, see [9] for details. The CDB ratio profile for HPT deformed Mg–10%Gd is plotted in Fig. 1. One can see a significant increase in CDB profile at low momentum region due to a strong contribution of positrons trapped at dislocations. On the other hand, there is no increase in the fraction of positrons annihilating with Gd electrons. It indicates no segregation of Gd atoms at dislocations or grain boundaries in HPT deformed sample.

4. Conclusions

A microstructure of HPT deformed Mg and Mg–10%Gd was characterized and compared with initial coarse grained materials. An incomplete dynamic recovery took place during HPT processing of Mg sample which resulted in a binomial type of structure. The HPT made Mg–10%Gd exhibits a homogeneous UFG microstructure with a high density of uniformly distributed dislocations and a grain size of about 100 nm. No microvoids and no segregation of Gd atoms at dislocations or grain boundaries were found. Both HPT deformed specimens exhibit a significantly increased microhardness compared to initial coarse-grained materials.

Acknowledgments

This work was supported by the Czech Grant Agency (contract 106/01/D049 and 106/05/0073), the Ministry of Education, Youth and Sports of Czech Republic (project 1K03025), and by DFG.

References

[1] B.L. Mordike, *Mater. Sci. Eng. A* **324**, 103 (2002).

[2] P. Vostrý, B. Smola, I. Stulíková, F. von Buch, B.L. Mordike, *Phys. Status Solidi A* **175**, 491 (1999).

[3] R.Z. Valiev, R.K. Islamgaliev, I.V. Alexandrov, *Prog. Mater. Sci.* **45**, 103 (2000).

[4] F. Bečvář, J. Čížek, L. Lešt'ak, I. Novotný, I. Procházka, F. Šebesta, *Nucl. Instrum. Methods A* **443**, 557 (2000).

[5] I. Procházka, I. Novotný, F. Bečvář, *Mater. Sci. Forum* **255-257**, 772 (1997).

[6] M.J. Puska, R.N. Nieminen, *J. Phys. F, Met. Phys.* **13**, 333 (1983).

[7] P. Hautojärvi, C. Corbel, in: *Proceedings of the International School of Physics "Enrico Fermi"*, Course CXXV, Eds. A. Dupasquier, A.P. Mills, IOS Press, Varena 1995, p. 491.

[8] M. Fahnle, B. Meyer, J. Mayer, J.S. Oehrens, G. Bester, in: *Diffusion Mechanisms in Crystalline Materials*, Ed. Y. Mishin, MRS Symposia Proceedings No. 527, p. 23.

[9] J. Čížek, I. Procházka, B. Smola, I. Stulíková, R. Kužel, Z. Matěj, V. Cherkaska, R.K. Islamgaliev, O. Kulyasova, *Mater. Sci. Forum* **482**, 183 (2005).